

High resolution infrared spectra of bulge globular clusters: Liller 1 and NGC 6553

Livia Origlia

Osservatorio Astronomico di Bologna, Via Ranzani 1, I-40127 Bologna, Italy

origlia@bo.astro.it

R. Michael Rich

Math-Sciences 8979, Department of Physics and Astronomy, University of California at Los Angeles, Los Angeles, CA 90095-1562

rmr@astro.ucla.edu

Sandra Castro

Palomar Observatory 105-24, California Institute of Technology, Pasadena, CA 91125

smc@astro.caltech.edu

Received _____; accepted _____

¹Data presented herein were obtained at the W.M.Keck Observatory, which is operated as a scientific partnership among the California Institute of Technology, the University of California, and the National Aeronautics and Space Administration. The Observatory was made possible by the generous financial support of the W.M. Keck Foundation.

ABSTRACT

Using the NIRSPEC spectrograph at Keck II, we have obtained echelle spectra covering the range $1.5 - 1.8 \mu\text{m}$ for 2 of the brightest giants in Liller 1 and NGC 6553, old metal rich globular clusters in the Galactic bulge. We use spectrum synthesis for the abundance analysis, and find $[\text{Fe}/\text{H}] = -0.3 \pm 0.2$ and $[\text{O}/\text{H}] = +0.3 \pm 0.1$ (from the OH lines) for the giants in both clusters. We measure strong lines for the alpha elements Mg, Ca, and Si, but the lower sensitivity of these lines to abundance permits us to only state a general $[\alpha/\text{Fe}] = +0.3 \pm 0.2$ dex. The composition of the clusters is similar to that of field stars in the bulge and is consistent with a scenario in which the clusters formed early, with rapid enrichment. We have difficulty achieving a good fit to the spectrum of NGC 6553 using either the low or the high values recently reported in the literature, unless unusually large, or no α -element enhancements are adopted, respectively.

Subject headings: Galaxy: bulge, globular clusters: individual (Liller 1, NGC 6553) — stars: abundances, late-type — techniques: spectroscopic

1. Introduction

With the growing awareness that the bulge globular clusters are a distinct subsystem has come a new urgency to determine their ages and chemical composition. To explore possible connections between clusters and the field, it is most interesting to compare the detailed compositions of these clusters with the Galactic bulge field population (McWilliam & Rich 1994). As simple stellar populations, these clusters also will play an important role in population synthesis for giant elliptical galaxies. At issue is determination of their iron and alpha element abundances from integrated light.

For many of these bulge clusters, foreground extinction is so great as to largely preclude optical studies of any kind, particularly at high spectral resolution. With the availability of NIRSPEC, a high throughput infrared echelle spectrograph at the Keck Observatory (McLean et al. 1998), comes the prospect of measuring the composition of the clusters in the bulge.

In this paper we present new, high resolution NIRSPEC spectra of bright giants in Liller 1 and NGC 6553. Both are relatively massive globular clusters ($M_V \sim -7.5$) lying 2.5 kpc from the Galactic Center (Harris 1999). This is the first in a series of papers which will address these globular clusters, the last major globular cluster subpopulation in the Galaxy for which high resolution abundances remain mostly to be determined.

Because of the relatively low extinction toward NGC 6553, this cluster has been widely studied and it is one of the few bulge clusters with a very secure turnoff age measurement. Ortolani et al. (1995) use WFPC2 turnoff photometry to demonstrate that NGC 6553 and the similarly metal rich cluster NGC 6528 are coeval with the well studied globular cluster 47 Tuc. A proper motion cleaned color-magnitude diagram of this cluster obtained using HST (Zoccali et al. 2001) cements the determination that this cluster is coeval with the Galaxy’s oldest populations. On the contrary, high extinction is present toward Liller 1. Its turnoff is not very well defined (Ortolani et al. 2001) but it is also likely to be old. Accurate abundance measurements of these old clusters give crucial insight into the process of early chemical enrichment in the bulge of our Galaxy.

In the last few years NGC 6553 and Liller 1 have been the subject of both optical and near infrared photometry (Ortolani, Bica & Barbuy 1996, Guarneri et al. 1998, Frogel, Kuchinski & Tiede 1995, Davidge 2000). Integrated spectra of their innermost core regions in the optical (Bica & Alloin 1986, Armandroff & Zinn 1988) and in the near infrared (Origlia et al. 1997; Frogel et al. 2001) are also available, while only for NGC 6553 have

optical spectra been obtained for individual red stars at both low (Minniti 1995; Coelho et al. 2001) and high resolution (cf. e.g. Barbuy et al. 1992; 1999, Cohen et al. 1999, Carretta et al. 2001).

Despite the relative large number of photometric and spectroscopic measurements, particularly in NGC 6553 (cf. e.g. Table 5 of Barbuy et al. 1999 for a summary), the inferred abundances are still somewhat discrepant, leaving open the question of the cluster actual metallicity. In particular the two most recent optical studies at high spectral resolution for members of NGC 6553 (cf. Barbuy et al. 1999, Carretta et al. 2001) disagree by 0.5 dex.

The near-IR spectral range is particularly suitable to study cool, metal rich and possibly heavily reddened stars of the bulge population. The importance of the infrared CO and OH bands as reliable carbon and oxygen abundance tracers in red giants had been known for a few decades (cf. e.g. Thompson et al. 1969; Thompson & Johnson 1974, Lambert et al. 1984, Kleinmann & Hall 1986, Wallace & Hinkle, 1996). More recently, such a diagnostics has been also used to study the metal content of the integrated red stellar population in globular clusters and early type galaxies (Origlia et al. 1997, Origlia 2000, Frogel et al. 2001) and to infer the oxygen abundance of some metal poor stars (Balachandran & Carney 1996, Meléndez, Barbuy Spite 2001).

Our observations and the infrared echelle spectra follow in Sect. 2. Sect. 3 discusses our abundance analysis, while in Sect. 4 the inferred metallicities and radial velocities are compared with previous results. Our concluding remarks are given in Sect. 5.

2. Observations and Data Reduction

We obtained near infrared, high-resolution echelle spectra of two bright giants in the cores of the bulge globular clusters Liller 1 and NGC 6553, on 26 July 2000. We used the infrared spectrograph NIRSPEC (McLean et al. 1998) which is equipped with an ALADDIN 1024×1024 InSb array detector and mounted at the Keck II telescope. The spectrograph employs a single echelle grating in quasi-littrow mode with a 5° out-of-plane angle and a lower resolution grating with a smaller blaze angle and zero out-of-plane angle as cross dispersor. The slit has a width of 0".43 (3 pixels) and a length of 12" and the nominal resolving power is $R=25,000$ (i.e. 12 km s⁻¹). We employed the standard NIRSPEC-5 setting, which uses the H-band filter and covers most of the 1.5-1.8 micron band with only small inter-order gaps.

The night of 26 July 2000 was photometric, but the dome rotation failed, permitting observations only of objects crossing through the dome slit, which fortunately lay nearly due South. We exposed for 3 × 10 min in Liller 1, and 2 × 10 min in NGC 6553. It must be assumed that a portion of the exposures were compromised by some occultation of the pupil by the dome. Considering that little time was available, it was fortunate that 2 bright giants in each cluster fell on the slit (without requiring image rotation). The 12" long slit was long enough to permit nodding between exposures. The H band images of the slit are given in Fig. 1; these were obtained using the slit viewing camera (SCAM) of NIRSPEC, which is equipped with a PICNIC 256×256 HgCdTe array detector and has a field of view of 46"×46" and a scale of 0".183 *pixel*⁻¹.

The raw frames were background subtracted and flat fielded. Each order of the echellogram has been then extracted and straightened according to its tilt angle. The normalized one-dimensional spectra have been obtained summing over the 3 brightest rows and dividing by the continuum, which was determined applying a low-pass smoothing filter

through each spectrum. Imperfect subtraction of some of the brightest OH night sky lines leaves some apparently high continuum points. Prior to fitting the final continuum, we overplotted the night sky spectrum and verified that these regions were spurious. The atmospheric absorption features have been removed using a reference O-star spectrum, but these are not significant, in any case. The inferred signal to noise (S/N) ratio of the final spectra is always ≥ 40 and the measured instrumental FWHM is $\approx 0.8 \text{ \AA}$.

The wavelength calibration uses the OH sky lines (Oliva & Origlia 1992); we compute a quadratic spline in the dispersion direction with an overall calibration accuracy of $\approx 0.16 \text{ \AA}$ or equivalently $\approx 3 \text{ km s}^{-1}$. The reduced echelle spectra of the observed stars in Liller 1 and NGC 6553, covering the 1.51-1.75 μm wavelength range, are shown in Figs. 2 and 3, respectively. The spectra of the two stars in each cluster are practically identical within the noise.

3. Abundance analysis

We compute suitable synthetic spectra of giant stars by varying the stellar parameters and the element abundances, using an updated version of the code described in Origlia et al. (1993) to obtain spectra in the whole 1-2.5 μm range. The computations use the LTE approximation and are based on the molecular blanketed model atmospheres of Johnson et al. (1980) which have been extensively used for abundance studies based on high resolution spectra of cool stars (e.g. Lambert et al. 1984; Smith & Lambert 1985, 1990). The atomic oscillator strengths and the excitation potentials have been taken from Kurucz's database. For the Ca lines around 1.615 μm we used the values tabulated by Bièmont & Grevesse (1973, hereafter BG73) which provide a more reasonable synthesis of the observed spectra (cf. Sec. 3.1 for a more quantitative analysis). The molecular oscillator strengths and excitation potentials have been computed as described in Origlia et al. (1993). The

reference Solar abundances have been updated according to Grevesse & Sauval (1999).

By using the CO ($\Delta v = 3$) and OH ($\Delta v = 2$) molecular lines in the 1.5-1.8 μm spectral window we can infer reliable carbon and oxygen abundances (cf. e.g. Lambert et al. 1984). These lines are not heavily saturated even in the high metallicity domain and still lie on the linear part of the element curve of growth, where the line equivalent width variation with the abundance is maximum. We can also infer an estimate of the nitrogen abundance using the CN ($\Delta v = -1$) molecular lines (cf. e.g. Sneden & Lambert 1982).

At the NIRSPEC resolution of $R=25,000$ we can measure several single rotation-vibration OH lines. However, our carbon abundances are mostly derived from CO bandheads; in contrast to OH, the CO lines are more blended at our resolution.

Other metal abundances can be derived from the atomic lines of Fe I, Mg I, Si I and Ca I, although heavily saturated and somewhat less sensitive to the element abundance variation compared to the molecular lines, being on the damping part of the curve of growth, where the equivalent width increases much more slowly with the element abundance.

The modeling of the main molecular and atomic lines for cool stars in the H band is relatively straightforward. The major source of continuum opacity is H^- and it has its minimum near 1.6 μm . These two facts also minimize any dependence of the results on the choice of model atmosphere. The molecular lines are due to rotation-vibration transitions in the ground electronic state, so they can be safely treated under the LTE approximation. At these low temperatures, the metals are mostly neutral or singly ionized, eliminating the need to compute equilibria for higher stages of ionization. The atomic oscillator strengths remain the major source of uncertainty, and their computed values could require a detailed cross-calibration with suitable stellar template spectra. In Sect. 3.1 we discuss in some more detail how different assumptions for the oscillator strength values can affect the line profiles and the derived element abundances.

From the near infrared (IR) photometry of Liller 1 and NGC 6553 published by Frogel, Kuchinski & Tiede (1995) and Guarneri et al. (1998), their $E(J-K)$ reddening of 1.70 and 0.41 and the corresponding $A_K=0.87$ and 0.24 corrections, and their distance moduli of $\mu_0=14.7$ and 13.6, respectively, we compute the $(J-K)_0$ colors and the absolute K magnitudes for the observed stars (cf. Table 1). We use the color-temperature transformation and the bolometric corrections of Montegriffo et al. (1995) specifically calibrated on globular cluster giants, to derive the stellar temperature and bolometric magnitudes of the observed stars from the $(J-K)_0$ color (cf. Table 1). The two giants in Liller 1 are the brightest in the cluster and we infer $T_{\text{eff}} \approx 3700$ and 3900 K, while those in NGC 6553 have $T_{\text{eff}} \approx 3900$ and 4000 K. The expected uncertainty in the temperature estimate is ≤ 200 K, taking into account the possible systematic effects due to the reddening correction and the color-temperature transformation. Concerning the stellar gravity, according to the theoretical evolutionary tracks, in the high metallicity domain the expected values for the stars in the upper part of red giant branch are $\log g \leq 1.0$, depending on their actual luminosity and temperature (see Origlia et al. 1997 and references therein for a more detailed discussion).

Both the photometric quantities reported in Table 1 and the similarity of the infrared spectra (cf. Figs. 2 and 3) indicate that the two observed stars in each clusters should have very similar photospheric parameters. Hence, as a first step in our analysis of the spectra, we adopt (cf. Table 2) average temperature and gravity of $T_{\text{eff}}=3800$ K and $\log g=0.5$ for the 2 giants of Liller 1 and $T_{\text{eff}}=4000$ K and $\log g=1.0$ for those in NGC 6553. We also adopt the microturbulence of $\xi = 2 \text{ km s}^{-1}$ according to the values inferred by Origlia et al. (1997) from the CO bandheads in the integrated spectra of these clusters. In Sec. 3.1, we will consider how our derived abundances depend on these parameters.

For both clusters the best fits to the observed spectra using the above reference stellar parameters have been obtained for half Solar $[\text{Fe}/\text{H}]$, Solar $[\text{O}/\text{Fe}]$ and a similar

enhancement by a factor of ≈ 2 for the other α elements (Si, Mg, Ca) (cf. Table 2). We also find some ^{12}C depletion and ^{14}N enhancement (by a factor of ≈ 2 , as well), as expected from the first dredge-up mixing process in the stellar interior during the evolution on the red giant branch (cf. e.g. Boothroyd & Sackmann 1999 for a recent review). The fit also gives the $^{12}\text{C}/^{13}\text{C} \leq 5$ ratio. Such a low value cannot be explained by first dredge-up alone and requires some extra-mixing processes occurring during the last ascent of the red giant branch (Boothroyd & Sackmann 1999 and references therein).

An overall, conservative estimate of the uncertainty in the derived absolute abundances is ≤ 0.2 dex. Our synthetic best fits superimposed on the observed spectra of Liller 1 and NGC 6553 in three major spectral regions of interest, are plotted in Figs. 4 and 5, respectively. These synthetic spectra well account for most of the observed features, and the few major discrepancies should be mainly ascribed to a bad OH sky line and/or atmospheric feature subtraction.

In such a high metallicity domain, it is almost impossible to find lines which are completely unblended, even at high resolution. Nevertheless, we identified a few representative metal and OH lines which are reasonably clean to provide useful equivalent width measurements. By integrating over a $\pm 1 \text{ \AA}$ range from the line central wavelength we obtain values systematically larger ($30 \pm 10\%$) than those from a simple gaussian fit of the line using the instrumental 0.8 \AA FWHM, possibly indicating that some blend effects are at work. For this reason we decided to use the values from the gaussian fit with an overall accuracy of $\pm 30 \text{ m\AA}$. These values are reported in Table 1.

The inferred heliocentric radial velocities (cf. Table 1) for the stars in Liller 1 (66 and 61 km s^{-1}) are consistent with the value listed by Harris (1996) ($52 \pm 15 \text{ km s}^{-1}$). In the case of NGC 6553 our velocities (-9 and -5 km s^{-1}) are well within the relative wide range of values (between -60 and $+60 \text{ km s}^{-1}$) published in the literature (cf. e.g. Table 3

of Coelho et al. 2001 for a summary).

3.1. Error budget

In order to investigate the influence of slightly different assumptions for the stellar parameters on the inferred abundances we also compute synthetic spectra with $\Delta A = \pm 0.2$ dex (where A is the input element abundance for the computation of the line opacities and the variation refers to all elements), $\Delta T_{\text{eff}} = \pm 200$ K, $\Delta \log g = \pm 0.5$ dex and $\Delta \xi = \pm 0.5$ km s⁻¹ with respect to the adopted reference parameters (cf. Table 2). The adopted ranges for the stellar parameters are quite conservative and somewhat representative of their maximum uncertainty. We analyze both the line profiles and the equivalent widths. The resulting stellar spectra of the two clusters, centered on a few selected atomic and molecular lines of interest are plotted in Figs. 6 and 7, while their measured equivalent widths are compared in Figs. 8 and 9, respectively .

A variation of ± 0.2 dex in the element abundance affects only slightly the depth and the broadening of the atomic line profiles, but strongly affects the more metal sensitive CO and OH lines. The change in the line strength due to a ± 0.2 dex abundance variation can be equally obtained by varying some other atmospheric parameters, but by quite a large amount. For example, ≥ 0.5 km s⁻¹ variation in the microturbulent velocity, and also temperature variation of ≥ 200 K in the case of the Ca and Si lines, could have a similar effect, but larger (smaller) microturbulent velocities and/or lower (higher) temperatures are required to fit lower (higher) input abundances, somewhat contrary to the stellar evolution prescriptions for population II stars (cf. e.g. Straniero & Chieffi 1991, Schaller et al. 1992, Bertelli et al. 1994, Cassisi et al. 1999).

The molecular bands behave in a similar fashion: the major change in the line strength

due to a ± 0.2 dex abundance variation, could also be the result of relatively large (± 0.5 dex) $\log g$ variation in the case of the CO band heads, while for the OH lines, somewhat more saturated, are mainly major temperature and microturbulent velocity variations which affect the line profiles. Again, as in the case of the atomic lines, a decrease in the input abundance has to be compensated for by lowering the stellar gravity and temperature or increasing the microturbulence velocity (viceversa for an increase of the input abundance). These trends are in the opposite direction of the standard evolution prescriptions along the red giant branch.

Line equivalent widths are only marginal affected (within the ± 30 mÅ scatter) by the variation of the stellar parameters in the ranges mentioned above, the major scatter ($\leq 2\sigma$) with the element abundance. In the case of the OH bands and the Si line (slightly blended with OH as well), a 200K increase in effective temperature with respect to the adopted reference gives model equivalent widths which are ($\geq 3\sigma$) lower than the observed widths. Although one might be concerned that the photometric estimate of the effective temperature can be quite uncertain (mainly due to reddening correction), the molecular lines are especially powerful in constraining its value. The scatter between the abundances inferred from different molecular lines (cf. e.g. the case of the two selected OH lines) is even smaller than the adopted ± 0.2 dex error, indicating that in presence of high signal to noise spectra the carbon and oxygen abundances can be constrained down to a limit of ± 0.1 dex.

It is also noteworthy that the stellar features under consideration show a similar trend with variations in the stellar parameters, although with different sensitivities. As a consequence of such a behavior, *relative* abundances are less dependent on stellar parameter variations. Moreover, the simultaneous fit of the different atomic and molecular bands in particular, requires more unique solutions for the adopted stellar parameters, significantly reducing their initial range of variation and ensuring a good self-consistency of the overall

spectral synthesis procedure.

On the basis of this analysis, we can conclude that minor stellar parameter variations in the proximity of their best fit solutions do not significantly affect (within ≈ 0.1 dex) the inferred abundances, and certainly do not affect the relative abundances.

As mentioned in Sect. 3, the adopted oscillator strength is an additional source of uncertainty in the abundances derived from the analysis of the atomic lines. In this respect, for some representative bright atomic lines in the H band we compared the results obtained using the oscillator strengths of the Kurucz’s list with those empirically calibrated by Meléndez & Barbuy (1999, hereafter MB99). On average, MB99 values are systematically lower but when the difference does not exceed 0.2 dex (which is the case for most of the atomic lines under consideration), both the line profiles and equivalent widths are only marginally affected and the overall scatter in the derived abundances is < 0.1 dex.

As an example, the atomic parameters and the inferred equivalent widths of the Ca, Fe, Si and Mg lines shown in Figs. 6, 7 and 8 (see also Table 1), adopting the Kurucz/BG73 or the MB99 oscillator strengths, respectively, for the two best fit models (cf. Table 2) to the observed spectra of Liller 1 and NGC 6553 are listed in Table 3 for comparison. The difference between the measured equivalent widths is generally $\leq 1\sigma$ (≤ 30 mÅ) with a small impact on the inferred element abundance (≤ 0.1 dex using the Ca $\lambda 1.61508$, Fe $\lambda 1.61532$ and Si $\lambda 1.58884$ lines, and ≤ 0.2 dex using the Fe $\lambda 1.55317$ and Mg $\lambda 1.57658$ lines). For the Ca $\lambda 1.61508$ line, if the larger oscillator strength by Kurucz ($\log\text{-gf} = 0.362$) is used, we must assume a significantly lower (≤ 0.5 dex) Ca abundance and an unlikely $[\text{Ca}/\text{Fe}] < -0.2$ dex underabundance.

4. Discussion

The red giant branch slope derived from optical (Ortolani, Bica & Barbuy 1996) and near-IR (Frogel, Kuchinski & Tiede 1995) color magnitude diagrams of Liller 1 suggest a supra-solar metallicity, although these estimates rely on extrapolation of empirical relations calibrated on less metal rich clusters. Integrated spectroscopy based on the calcium triplet (Armandroff & Zinn 1988) also suggests twice the Solar metallicity. More recently, color-magnitude diagrams from near-infrared photometry (Davidge 2000), and integrated spectroscopy of the CO feature around $1.6 \mu\text{m}$ (Origlia et al. 1997) are both consistent with half solar metallicity. Our present near IR high resolution spectra of the two single giants confirm such a sub-solar value. Davidge (2000) also finds that stars in Liller 1 are not as metal rich as those in the surrounding bulge. Frogel, Kuchinski & Tiede (1995) also noticed that the stars in the surrounding field of Liller 1 are redder than the most likely cluster members but since they were not able to solve the ambiguity between possible abundance or reddening variations, they did not use this external field to decontaminate the cluster color-magnitude diagram. Ortolani, Bica & Barbuy (1996) do not perform a detailed field decontamination of their optical color-magnitude diagrams, however they suggest that the cluster stars can be as metal rich as the bulge population given the locus and curvature of the red giant branch.

The most recent photometric and spectroscopic estimates of the metallicity of NGC 6553 range between one fifth (Cohelo et al. 2001) and almost Solar values (Carretta et al. 2001). The two most recent sets of high resolution spectroscopic measurements in the optical range (Barbuy et al. 1999 and Cohen et al. 1999) give $[\text{Fe}/\text{H}]=-0.55$ by measuring 2 bright giants and $[\text{Fe}/\text{H}]=-0.16$ by measuring 5 red horizontal branch stars, respectively. Carretta et al. (2001) propose a revised iron abundance of $[\text{Fe}/\text{H}]=-0.06$ for NGC 6553, using the same spectra and measured equivalent widths. Our iron abundance estimate

based on bright giants as well, is somewhat in between the values proposed by Barbuy et al. (1999) and by Cohen et al. (1999) as revised by Carretta et al. (2001). An overall excess of α -elements (by a factor of ≈ 2) is found by all the high resolution studies.

Figure 10 shows that we cannot achieve a good fit using the iron abundances recently reported in the literature. We compare our observations with synthetic spectra, produced for the two different iron abundances reported by Barbuy et al. (1999) and by Cohen et al. 1999 (adopting the suggested revision of Carretta et al. (2001) and $[\alpha/\text{Fe}] = +0.3$ in both cases). Iron abundances as low as proposed by Barbuy et al. (1999) or higher as proposed by Carretta et al. (2001) can still be barely consistent with our observed iron line strengths, but they would not optimize our fit. Moreover, as shown in Fig. 11 also the difference between the line equivalent widths as measured in the model and observed spectra can exceed the 1σ scatter. Most significantly, both measurements would be *inconsistent* with an $[\alpha/\text{Fe}]$ enhancement by $+0.3$ dex (found by both groups, and present in the Galactic bulge field). If $[\text{Fe}/\text{H}] = -0.6$, then we need to assume $[\text{C}/\text{Fe}] \approx 0.0$ and an $[\alpha/\text{Fe}]$ enhancement ≥ 0.5 dex to account for line strengths and equivalent widths of the CO, OH and the other alpha elements, while if $[\text{Fe}/\text{H}] = -0.1$, a higher carbon depletion and only a marginal (if any) $[\alpha/\text{Fe}]$ enhancement is required. Note that our finding of Solar oxygen abundance from the OH lines should be indeed rather firmly settled within ± 0.1 dex (cf. Sect. 3.1).

The discrepancy in the inferred abundances among these different data sets seem most likely due to systematic abundance analysis effects rather than being related to the evolutionary stage of the observed stars (cf. Coelho et al. 2001). In this respect, it is also interesting to compare our oxygen abundance in NGC 6553 with that of Cohen et al. (1999), where the 9 ev lines of the triplet at 7774\AA are used (with non-LTE corrections). Cohen et al. find $[\text{O}/\text{Fe}] = +0.50 \pm 0.2$, but each of their four stars exceeds our value of $[\text{O}/\text{Fe}]$, with one star at $[\text{O}/\text{Fe}] = +0.68$. Nevertheless, these permitted oxygen lines of high-excitation

potential seem to produce some artificial over-enhancement (by a factor of few) in the derived abundance compared to that one derived from the forbidden [OI] 6300Å lines (cf. e.g. Meléndez, & Barbuy 2001 and references therein). Considering the importance of oxygen in chemical evolution, and as an indicator of the star formation history, it will be valuable to extend these comparisons over the full range of iron abundance.

Our findings are consistent with recent abundance determinations for field stars in the Galactic bulge (Rich & McWilliam 2000), for which $[O/Fe] \approx +0.3$ at $[Fe/H]=0$ using the forbidden oxygen line at 6300 Å. According to the long-held paradigm that massive star supernovae mainly produce alpha elements (cf. reviews by Wheeler, Sneden, & Truran 1989 and McWilliam 1997), our abundance patterns in NGC 6553 and Liller 1 add one more piece of evidence consistent with early and rapid bulge formation (cf. e.g. Matteucci, Romano & Molaro 1999, Wyse 2000).

However, our findings for NGC 6553 and Liller 1 may not be generally applicable to the bulge globular clusters; there is clearly much work to be done. Consider the case of NGC 6528, which Ortolani et al. (1995) find to have an age identical to that of NGC 6553. The abundance analysis of four red horizontal branch stars in NGC 6528 by Carretta et al. 2001 finds $[Fe/H]=+0.07$, with Solar oxygen abundance and mild α - element enhancement. The oxygen abundance in NGC 6528 is measured from the 6300Å forbidden line and the carbon abundance is poorly constrained. Nonetheless, the need for more studies of bulge globular clusters is clear, and the use of both optical and infrared spectroscopy could help to settle some of the discrepant abundance determinations (e.g. combining CNO abundances from the infrared with optical measurements of other elements).

5. Conclusions

Using the NIRSPEC spectrograph at Keck II, we have obtained H-band echelle spectra at $R = 25,000$ of two of the brightest giants in each of the Galactic bulge globular clusters NGC 6553 and Liller 1. Employing spectrum synthesis, we find $[\text{Fe}/\text{H}] = -0.3 \pm 0.2$ and $[\text{O}/\text{H}] = +0.3 \pm 0.1$ for the giants in both clusters. We measure strong lines for the α -elements Mg, Ca, and Si, but the lower sensitivity of these lines to abundance permits us to only state a general $[\alpha/\text{Fe}] = +0.3 \pm 0.2$ dex. The oxygen abundance is based on many lines in the OH spectrum, rather than on the single forbidden line at 6300 \AA , or the 9 ev triplet at 7774 \AA . Ours is the first use of the OH lines to measure $[\text{O}/\text{H}]$ in old, metal rich stellar populations. Our finding that oxygen is enhanced relative to iron is consistent with massive star supernovae being responsible for the enrichment, and it is noteworthy that alpha enhancements are securely determined in old stars with a high iron abundance of $[\text{Fe}/\text{H}] = -0.3$.

Our abundances for these two ancient globular clusters strengthens further the link between the bulge globular clusters and the bulge field population, pointing toward early formation and rapid enrichment for both clusters and field.

RMR acknowledges support from grant number AST-0098739, from the National Science Foundation. The authors are grateful to telescope operator Terry Stickel, whose competence and encouragement in the face of technical difficulties made these observations possible. We are also grateful to the staff at the Keck observatory and to Ian McLean and the NIRSPEC team. The authors wish to extend special thanks to those of Hawaiian ancestry on whose sacred mountain we are privileged to be guests. Without their generous hospitality, none of the observations presented herein would have been possible.

REFERENCES

- Armandroff, T. E., & Zinn, R. 1988, *AJ*, 96, 588
- Balachandran, S. C., & Carney, B. W 1996, *AJ*, 111, 946
- Barbuy, B., Castro, S., Ortolani, S., & Bica, E. 1992, *A&A*, 259, 607
- Barbuy, B., Renzini, A., Ortolani, S., Bica, E., & Guarnieri, M. D. 1999, *A&A*, 341, 539
- Bertelli, G., Bressan, A., Chiosi, C., Fagotto F., & Nasi, E. 1994, *A&AS*, 106, 27
- Bica, E., & Alloin, D. 1986, *A&A*, 162, 21
- Bièmont, E., & Grevesse, N. 1973, *Atomic Data and Nuclear Data Tables*, 12, 221 (BG73)
- Boothroyd, A. I., & Sackmann, I. J. 1999, 1999, *ApJ*, 510, 232
- Carretta, E., Cohen, J., Gratton, R.G., & Behr, B. 2001, *AJ*, 122, 1469
- Cassisi, S., Castellani, V., Degli’Innocenti, S., iSalaris, M., & Weiss, A. 1999, *A&AS*, 134, 103
- Cohen, J. G., Gratton, R. G., Behr, B. B., & Carretta, E. 1999, *ApJ*, 523, 739
- Coelho, P., Barbuy, B., Perrin, M. N., Idiart, T., Schiavon, R. P., Ortolani, S., & Bica, E. 2001, *A&A*, 376, 136
- Davidge, T. J. 2000, *ApJS*, 126, 105
- Frogel, J. A., Kuchinski, L. E., & Tiede, G. P. 1995, *AJ*, 109, 1154
- Frogel, J. A., Stephens, A. W., Ramirez, S., & DePoy, D. L. 2001, *AJ*, submitted
- Guarnieri, M. D., Ortolani, Montegriffo, P., Renzini, A., Barbuy, B., Bica, E., & Moneti, A. 1998, *A&A*, 331, 70
- Grevesse, N., & Sauval, A. J. 1999, *Space Science Reviews*, 85, 161
- Harris, W. E. 1996, *AJ*, 112, 1487

- Harris, W.E. 1999, <http://www.physics.mcmaster.ca/Globular.html>
- Johnson, H. R., Bernat, A. P., & Krupp, B. M. 1980, ApJS, 42, 501
- Kleinmann, S. G., & Halli, D. N..B.x, 1986, ApJS, 62, 501
- Lambert, D. L., Brown, J. A., Hinkle, K. H., & Johnson, H. R. 1984, ApJ, 284, 223
- Matteucci, F., Romano, D., & Molaro, P. 1999, A&A, 341, 458
- McLean, I. et al. 1998, SPIE, 3354, 566
- McWilliam, A., & Rich, R.M. 1994, ApJS, 91, 749
- McWilliam, A. 1997, ARA&A, 35, 503
- Meléndez, J., & Barbuy, B. 1999, ApJS, 124, 527 (MB99)
- Meléndez, J., Barbuy, B., & Spite, F. 2001, ApJ, 556, 858
- Minniti, D. 1995, A&AS, 113, 299
- Montegriffo, P., Ferraro, F.R., Fusi Pecci, F., & Origlia, L., 1995, MNRAS, 276, 739
- Oliva, E., & Origlia, L. 1992, A&A, 280, 536
- Origlia, L., Moorwood, A. F. M., & Oliva, E. 1993, A&A, 280, 536
- Origlia, L., Ferraro, F. R., Fusi Pecci, F., & Oliva, E. 1997, A&A, 321, 859
- Origlia, L. 2000, in *The Evolution of the Milky Way*, ed. F. Matteucci, & F. Giovannelli, Kluwer Academic Publishers, 221
- Ortolani, S., Renzini, A., Gilmozzi, R., Marconi, G., Barbuy, B., Bica, E., & Rich, R.M. 1995, Nature, 377, 701
- Ortolani, S., Bica, E., & Barbuy, B. 1996, A&A, 306, 134
- Rich, R.M., & McWilliam, A. 2000, SPIE, 4005, 150
- Schaller, G., Schaerer, D., Meynet, G., & Maeder, A. 1992, A&AS, 96, 269

- Smith, V. V., & Lambert, D. L. 1985, *ApJ*, 294, 326
- Smith, V. V., & Lambert, D. L. 1990, *ApJS*, 72, 387
- Snedden, C., & Lambert, D. L. 1982, *ApJ*, 259, 381
- Thompson, R. I., Schnopper, H. W. Mitchell, R. I., & Johnson, H. L. 1969, *ApJ*, 158, 117
- Thompson, R. I., & Johnson, H. L. 1974, *ApJ*, 193, 147
- Wallace, L., & Hinkle, K. 1996, *ApJS*, 107, 312
- Wheeler, J.C., Sneden, C., & Truran, J.W. 1989, *ARA&A*, 27, 279
- Wyse, R. F. G. 2000, *Ap&SS*, 267, 145
- Zoccali, M., Renzini, A., Ortolani, S., Bica, E., & Barbuy, B. 2001, *AJ*, 121, 2638

Table 1. $(J-K)_0$ colors, heliocentric radial velocity and line equivalent widths (mÅ) for the observed stars in Liller 1 and NGC 6553.

	Liller 1 #1	Liller 1 #2	NGC 6553 #1	NGC 6553 #2
ref # ^a	1	2	40201	47192
$(J-K)_0^a$	1.04	0.93	0.93	0.86
$M(K)_0^a$	-6.91	-6.28	-4.87	-5.09
M_{bol}^a	-4.11	-3.68	-2.27	-2.59
v_r [km s ⁻¹]	66	61	-9	-5
Ca λ 1.61508	316	310	274	254
Fe λ 1.61532	218	243	237	229
Fe λ 1.55317	209	186	196	184
Mg λ 1.57658	417	418	435	437
Si λ 1.58884	505	487	496	494
OH λ 1.55688	307	295	269	251
OH λ 1.55721	321	307	288	279

Note. — ^a Stars in Liller 1 from Frogel, Kuchinski & Tiede (1995), in NGC 6553 from Guarnieri et al. (1998).

Table 2. Adopted stellar atmosphere parameters.

	Liller 1 #1	Liller 1 #2	NGC 6553 #1	NGC 6553 #2
T_{eff}	3800	3800	4000	4000
$\log g$	0.5	0.5	1.0	1.0
ξ [km s ⁻¹]	2	2	2	2
[Fe/H]	-0.3	-0.3	-0.3	-0.3
[α /Fe]	+0.3	+0.3	+0.3	+0.3
[C/Fe]	-0.3	-0.3	-0.3	-0.3

Table 3. Atomic line modeling: excitation potentials (eV), oscillator strengths and equivalent widths (mÅ).

Line	χ (eV)	log-gf			EW (mÅ)		
		Kurucz ^a	mod1 ^b	mod2 ^c	MB99	mod1 ^b	mod2 ^c
Ca λ 1.61508	4.53	-0.190	304	284	-0.34	294	271
Fe λ 1.61532	5.35	-0.821	252	237	-0.82	252	237
Fe λ 1.55317	5.64	-0.357	202	206	-0.73	168	169
Mg λ 1.57658	5.93	0.380	424	437	0.07	391	405
Si λ 1.58884	5.08	-0.030	504	485	-0.25	495	474

Note. —

^a For the Ca line the log-gf value is taken from BG73.

^b Best fit model to the observed spectra of Liller 1 (cf. Table 2).

^c Best fit model to the observed spectra of NGC 6553 (cf. Table 2).

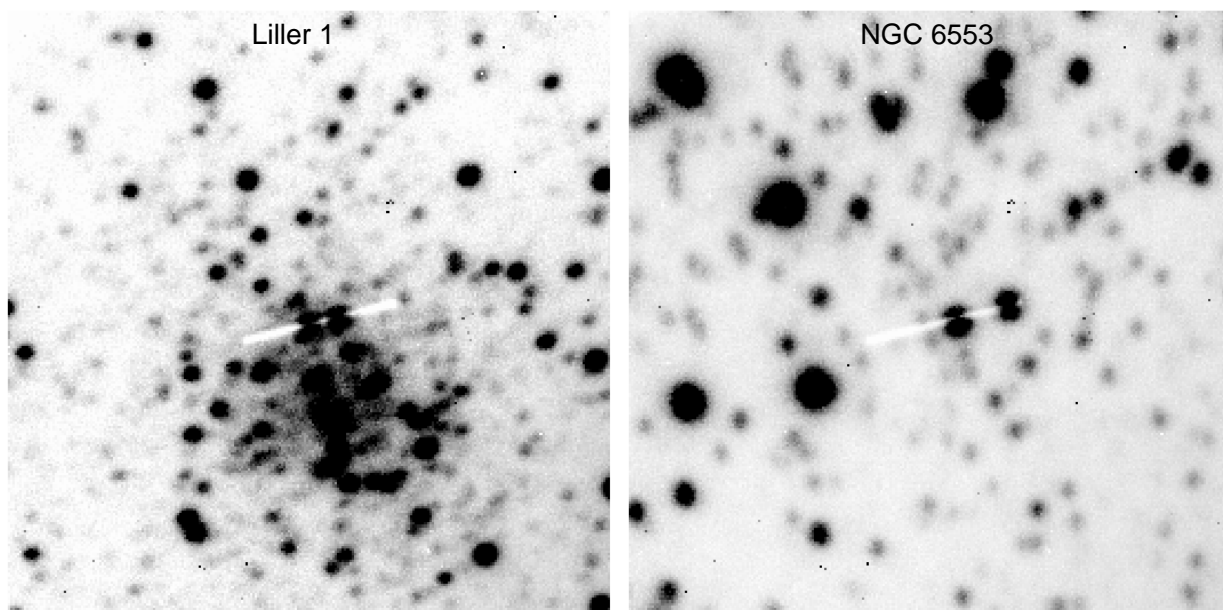


Fig. 1.— H band images of the fields in the cores of Liller 1 and NGC 6553 as imaged by the slit viewing camera (SCAM) of NIRSPEC. The field of view is $46''$ on a side (North up, East to the left), and the image scale is $0''.183 \text{ pixel}^{-1}$; the slit is $12''$ long.

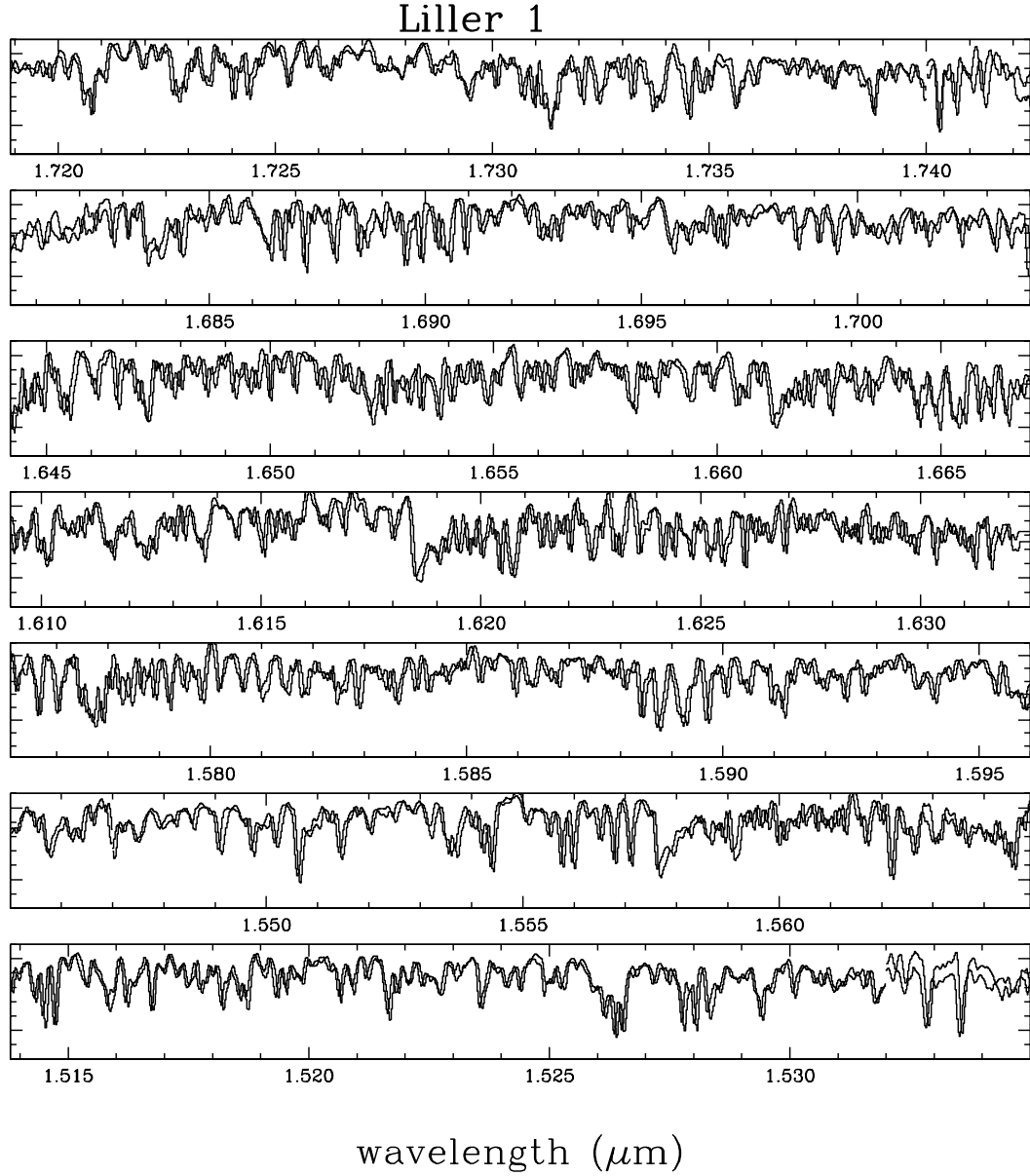


Fig. 2.— Normalized echelle spectra in the 1.51-1.75 μm wavelength range of the two giant stars in Liller 1.

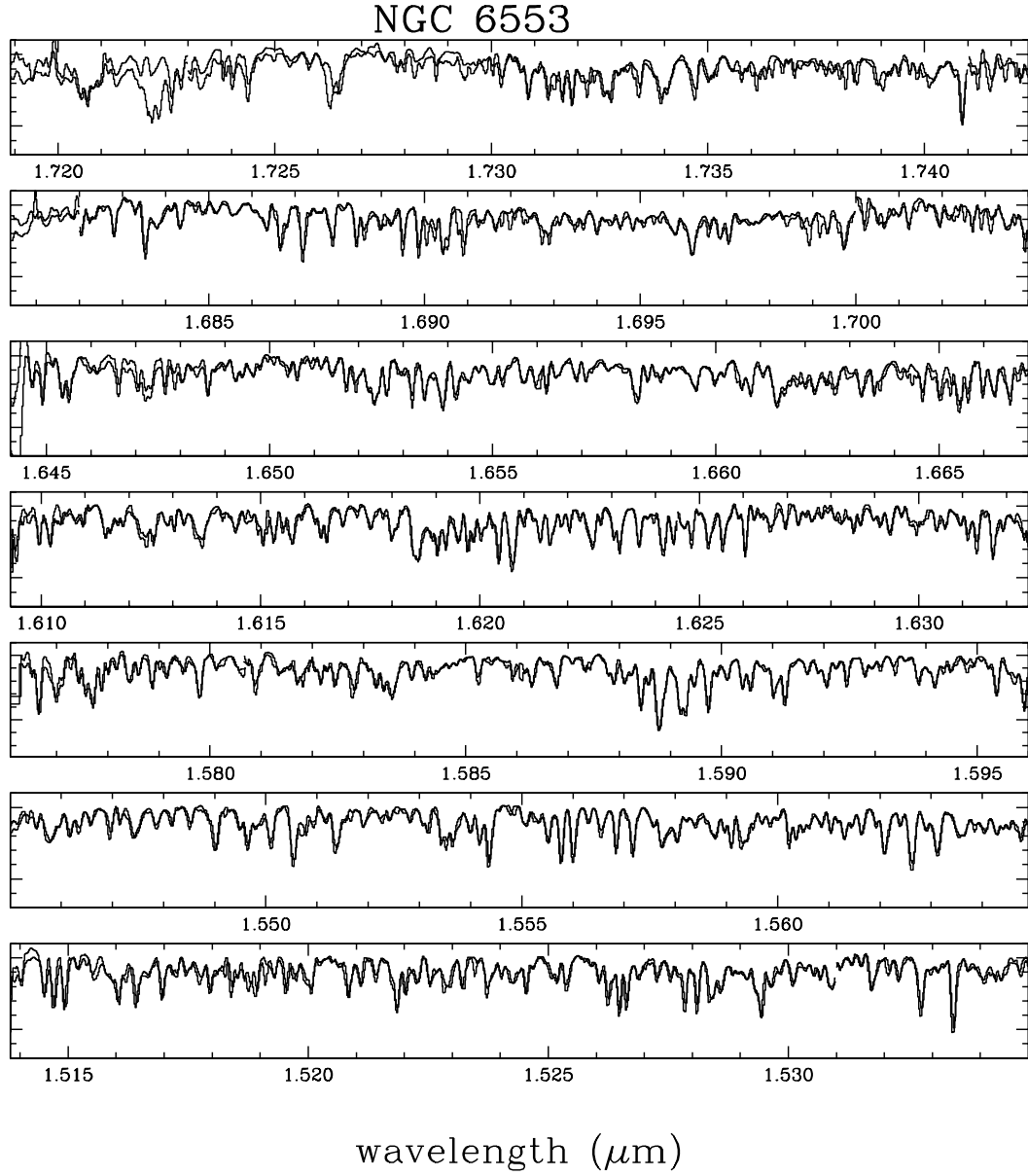


Fig. 3.— As in Fig. 2 but for the two giant stars in NGC 6553.

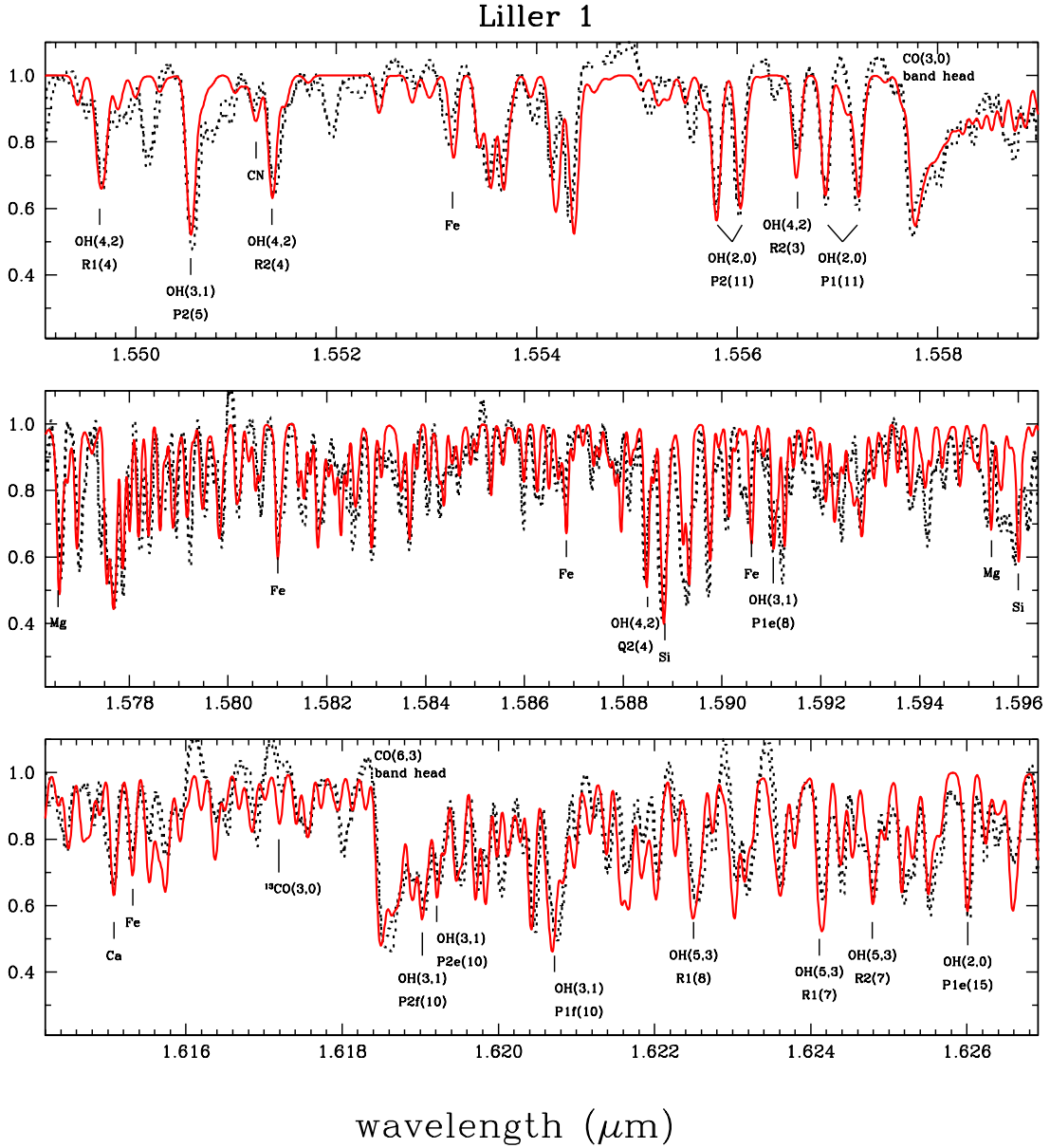


Fig. 4.— Selected portions of the observed echelle spectra (dotted lines) of the two giants in Liller 1 with our best fit synthetic spectrum (solid line) superimposed. A few important molecular and atomic lines of interest are marked. Most of these observed feature are well fitted by our synthetic spectrum and the few major discrepancies can be mainly ascribed to poor subtraction of overlying OH emission lines in the sky (see also Sect. 3). The derived abundances are based on a fit of the synthetic spectrum to all three orders of the spectrum.

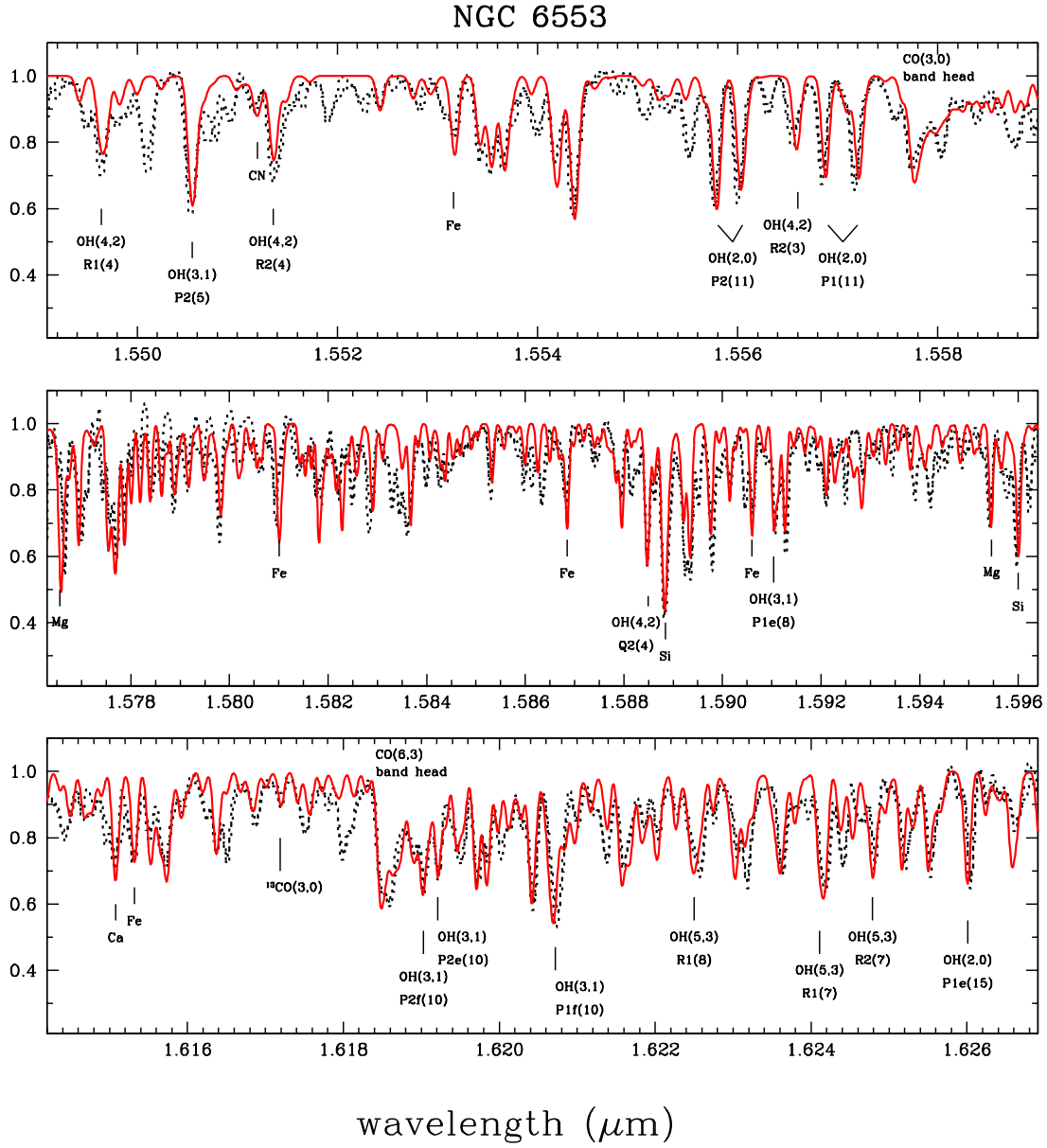


Fig. 5.— As in Fig. 4 but for the two giant stars in NGC 6553.

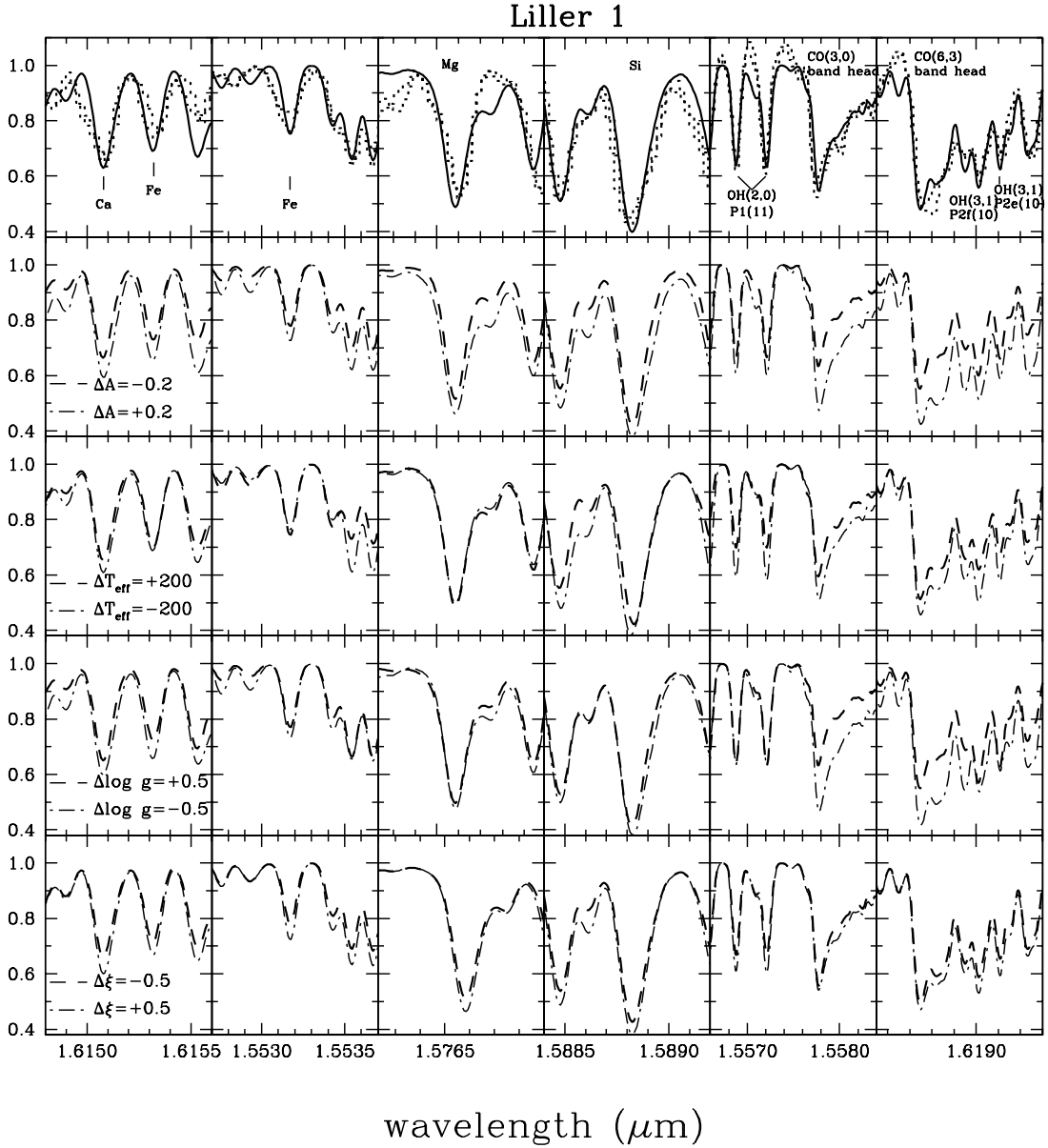


Fig. 6.— Spectra centered on a few atomic and molecular features of interest. Top panels: observed spectra of the two giants in Liller 1 (dotted lines) and our best fit (solid line), using $T_{\text{eff}}=3800$ K, $\log g=0.5$, $\xi=2$ km s $^{-1}$, $[\text{Fe}/\text{H}]=-0.3$, $[\alpha/\text{Fe}]=+0.3$, $[\text{C}/\text{Fe}]=-0.3$ as reference stellar parameters. Below, from the top to the bottom: synthetic spectra with $\Delta A=\pm 0.2$ dex, $\Delta T_{\text{eff}}\mp 200$ K, $\Delta \log g=\mp 0.5$ and $\Delta \xi\pm 0.5$ km s $^{-1}$ with respect to the above reference parameters (cf. also Table 2).

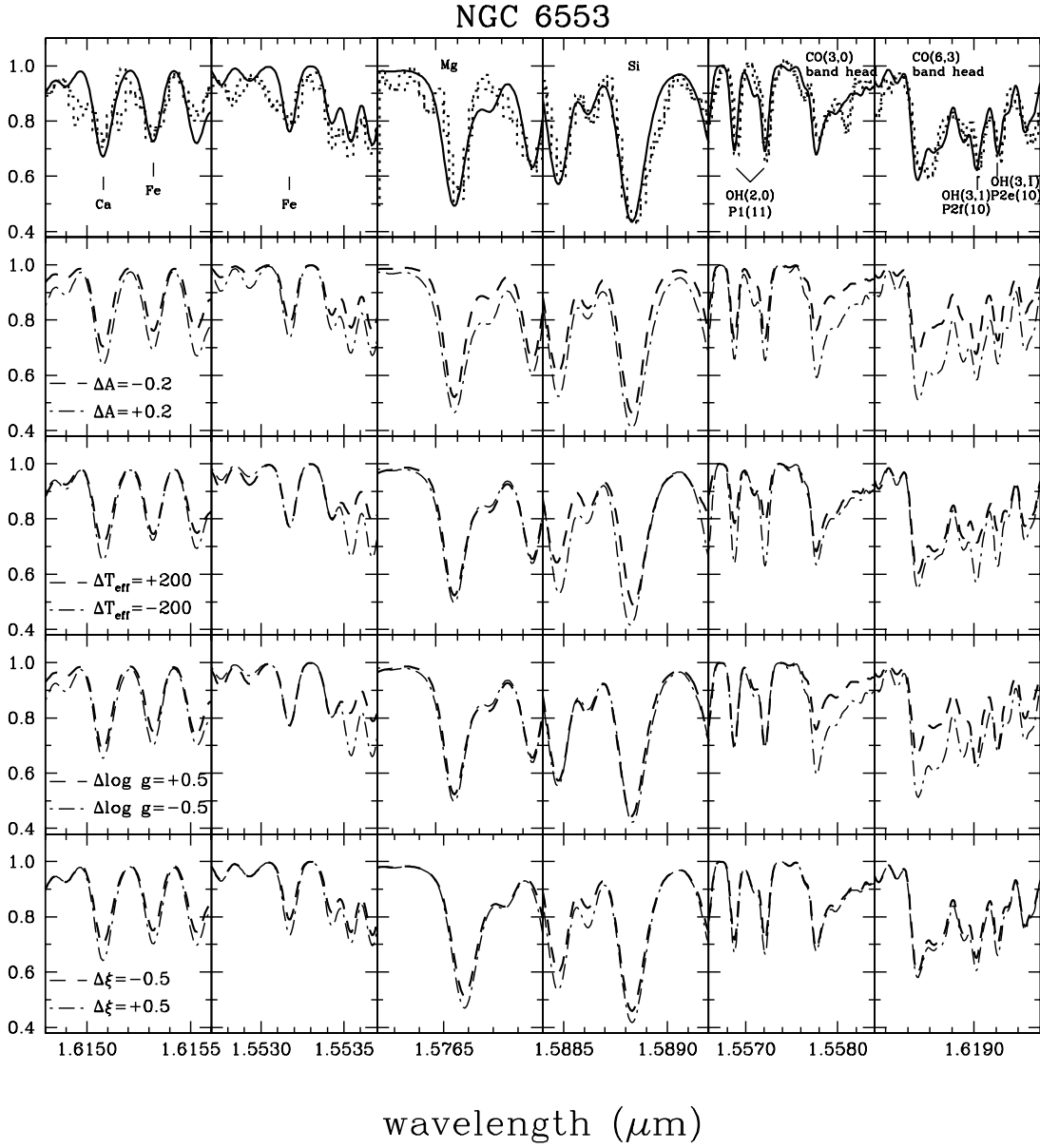


Fig. 7.— As in Fig. 6, but for the stars in NGC 6553 and $T_{\text{eff}}=4000$ K, $\log g=1.0$ reference temperature and gravity.

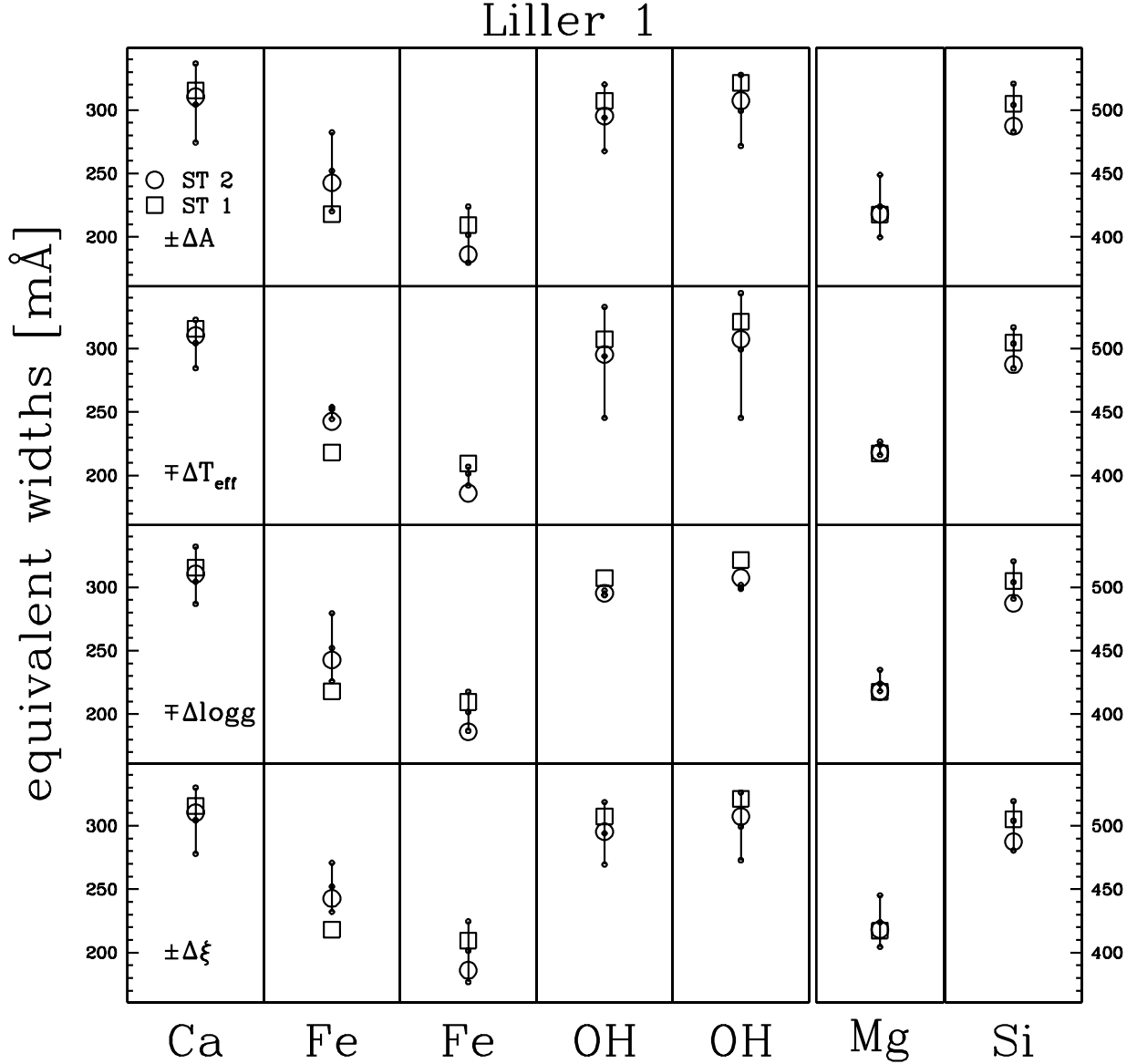


Fig. 8.— Liller 1 : measured equivalent widths for the selected atomic and molecular features from the observed (symbols) and synthetic (dots connected by vertical lines) spectra plotted in Fig. 6 with varying the stellar parameters. The central dot refers to the models with the the reference parameters listed in Table 2, while the top and bottom dots refer to models with $\Delta A = \pm 0.2$ dex, $\Delta T_{\text{eff}} = \pm 200$ K, $\Delta \log g = \pm 0.5$ and $\Delta \xi = \pm 0.5$ km s⁻¹ with respect to the reference one.

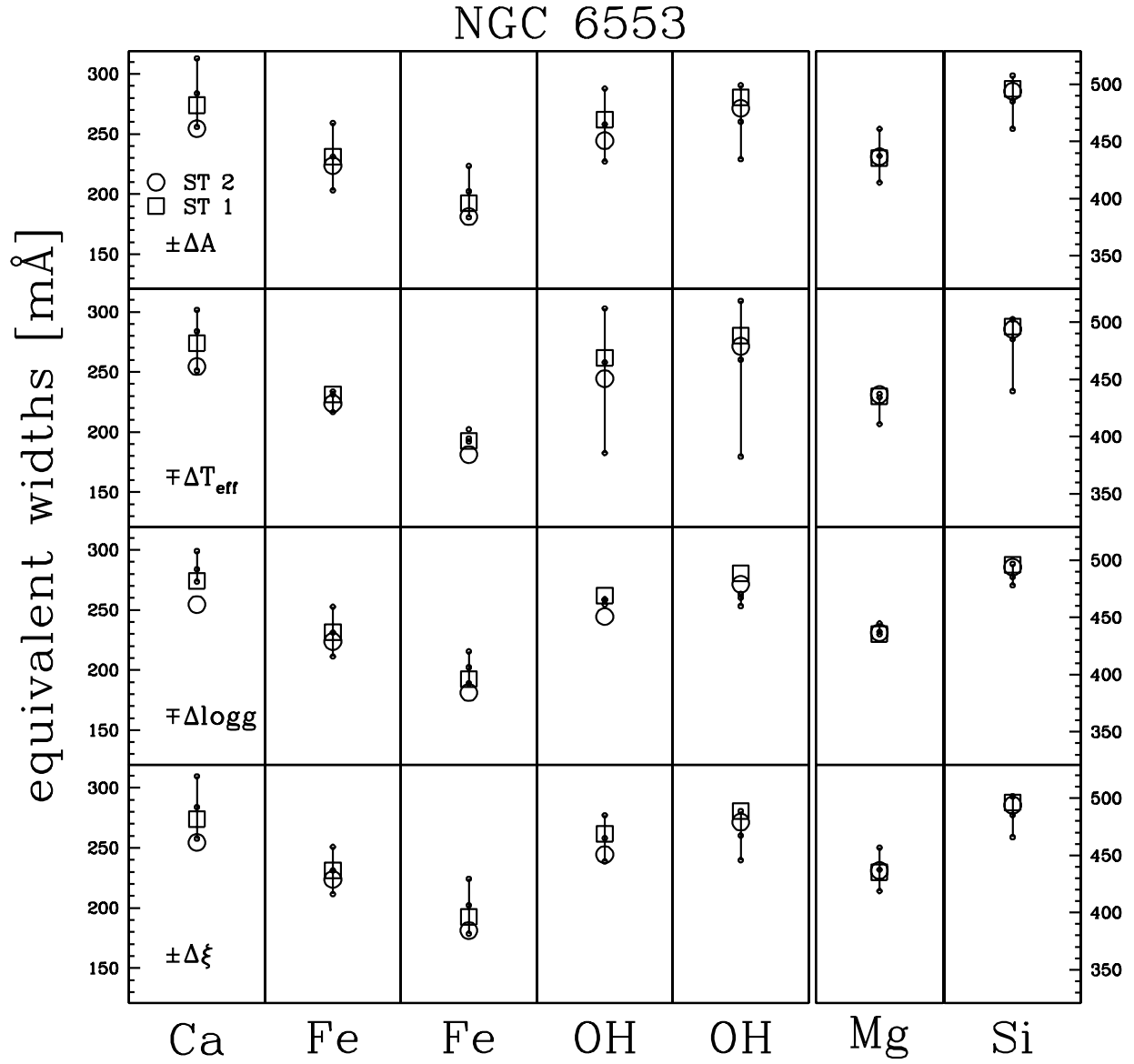


Fig. 9.— As in Fig. 8, but for the stars and in NGC 6553 and the synthetic spectra plotted in Fig. 7.

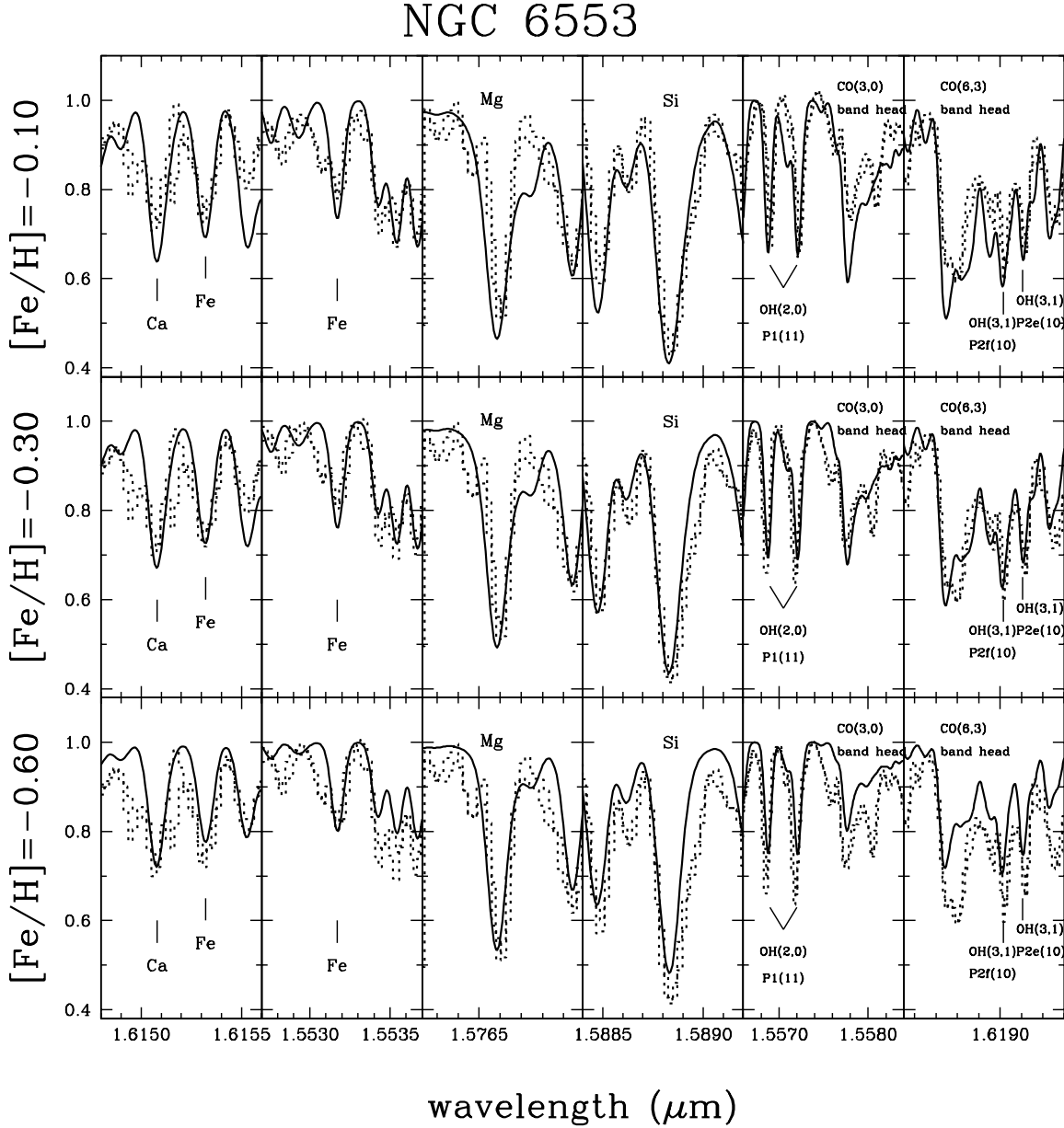


Fig. 10.— Observed spectra of the two giants in NGC 6553 (dotted lines) and our best fits (full lines) assuming a metal rich composition of $[\text{Fe}/\text{H}] = -0.1$ (top panel), $[\text{Fe}/\text{H}] = -0.3$ (middle panel) and $[\text{Fe}/\text{H}] = -0.6$ (bottom panel). The other stellar parameters are as in Table 2. These plots show that our $[\text{Fe}/\text{H}] = -0.3$ and $[\alpha/\text{Fe}] = +0.3$ abundances (middle panels) are well constrained. An abundance significantly lower than ours gives an especially poor fit to the data.

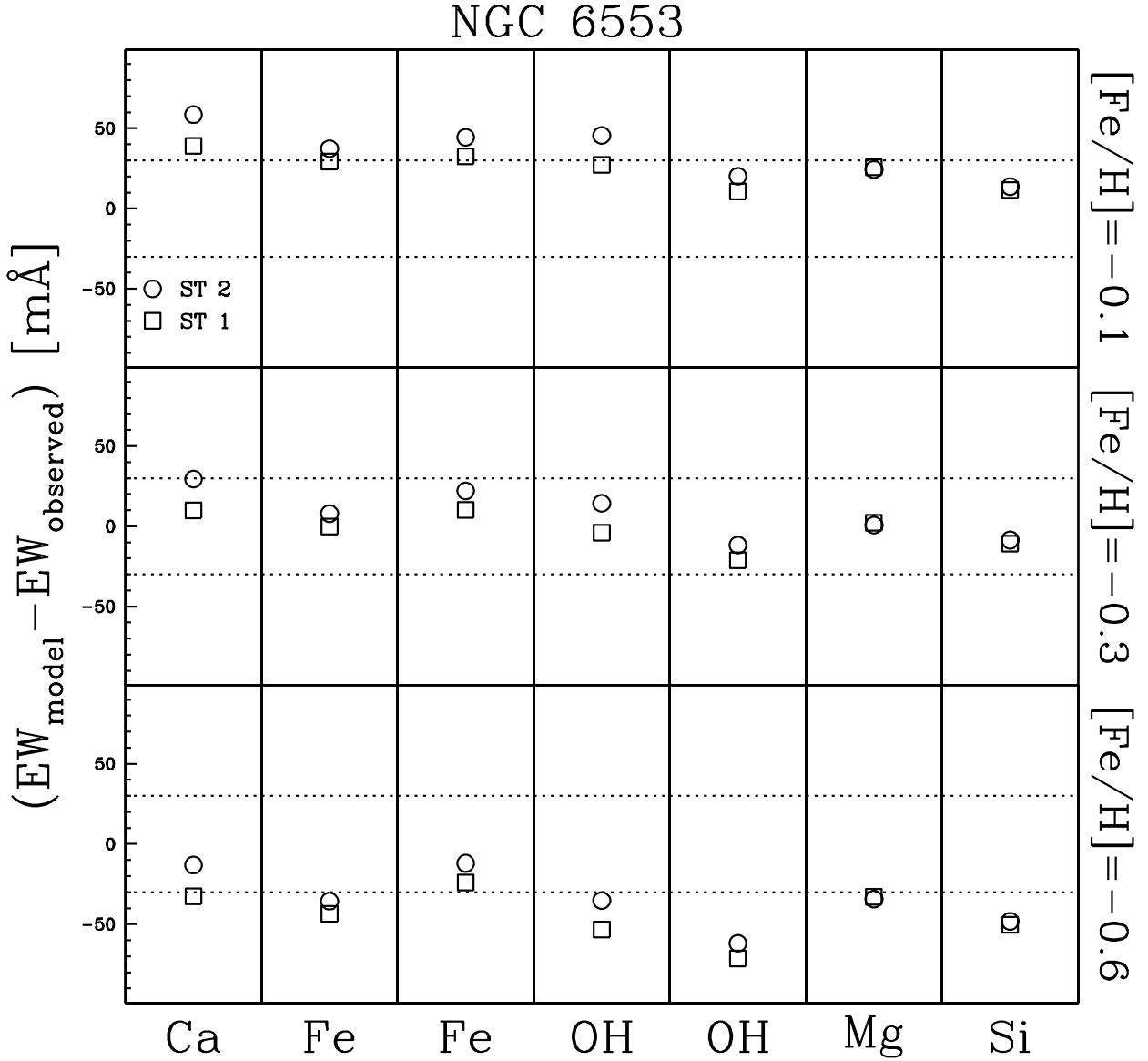


Fig. 11.— Difference between the line equivalent width measured in the models and in the observed spectra of the two giants in NGC 6553, assuming a metal rich composition of $[\text{Fe}/\text{H}] = -0.1$ (top panel), $[\text{Fe}/\text{H}] = -0.3$ (middle panel) and $[\text{Fe}/\text{H}] = -0.6$ (bottom panel). The other stellar parameters are as in Table 2. The dotted lines indicate the $\pm 1\sigma$ scatter. Using our $[\text{Fe}/\text{H}] = -0.3$ and $[\alpha/\text{Fe}] = +0.3$ abundances (middle panels) the difference between the equivalent widths of the model and the observed spectra is always $< 1\sigma$, while increases especially for an abundance significantly lower than ours.